

One-pot, Three Component, and Green Synthesis of 2-(Aryl)-3-((2-oxo-2-(2-oxo-2H-chromen-3-yl)ethyl)amino)imidazolidin-4-one Derivatives using Graphene Oxide Nanosheets under Microwave Irradiation: A Comparison Study Between One-pot and Step by Step Synthesis

Sajid Maksad Radhi^{a*}, Ban Hasan Taresh^b, Nesser Kadham Shareef^a, and Luma Majeed Ahmed^{a*}

a) Department of chemistry, College of Science, University of Kerbala, Kerbala, Iraq

b) Department of Clinical Laboratories, College of Applied Medical Sciences, University of Kerbala, Kerbala, Iraq

Received 20 May 2022; received in revised form 23 July 2022; accepted 20 September 2022 (DOI: 10.30495/IJC.2022.1959181.1937)

ABSTRACT

In this study, two different methods were described for the synthesis of 2-(aryl)-3-((2-oxo-2-(2-oxo-2H-chromen-3-yl)ethyl)amino)imidazolidin-4-one derivatives under microwave irradiation. The first method was step by step method. In step by step method, 3-(2-hydrazinylacetyl)-2H-chromen-2-one and aromatic aldehydes in 1 mL of absolute ethanol were irradiated with appropriate power within 3-10 min to obtain imine products. Then, the imine products were isolated and reacted with glycine to produce the 2-(aryl)-3-((2-oxo-2-(2-oxo-2H-chromen-3-yl)ethyl)amino)imidazolidin-4-one under microwave irradiation. In the one-pot method, the graphene oxide nanosheets were applied as heterogeneous catalysts. Hence, the graphene oxide nanosheets were synthesized based on Hummer's method. The catalyst was characterized by field emission scanning electron microscopy (FE-SEM), Fourier transform infrared spectroscopy (FT-IR), Raman spectroscopy, and X-ray diffraction (XRD) techniques. Then, 3-(2-hydrazinylacetyl)-2H-chromen-2-one, glycine, and aromatic aldehydes were irradiated using microwave irradiation in the presence of 0.5 mol% of graphene oxide nanosheets in ethanol. The prepared catalyst showed superior reusability for seven catalytic cycles. Our results showed that the one-pot method was better than the step by step method.

Keywords: Graphene oxide; one-pot; imidazolidine; microwave; synthesis; catalyst

1. Introduction

The benzopyran-2-one (coumarin or chromen-2-one) ring unit, which is present in natural materials (like warfarin drug) with interesting pharmacological properties, makes chemical and medical scientists interested for several decades in finding the natural coumarins or synthetic analogs for their applicability as drugs [1]. Some of the molecules based on the coumarin unit system have displayed different drug properties (**Fig. 1**). The different synthetic routes have led to interesting derivatives including warfarin, scoparone, armillarasin A, osthole, agasyllin, and methoxalen which have been found to be useful in medicinal, anti-HIV therapy, and antitumor, as well as anti-

inflammatory. Some coumarins have displayed inhibitory activities in breast cancer chemotherapy [2]. Coumarin-estrogen conjugates and coumarin receptor modulators have been described as potential anti-breast cancer agents [2]. There is a strong interest to explore potential new drugs based on coumarin for breast cancer since breast cancer is the most cause of death in American women.

As coumarin ring systems have proven to be effective pharmaceutical drugs, there is a growing demand for their synthesis and application in different fields of sciences. Many methods have been used for application as starting materials and different reaction conditions (**Scheme 1**). This Scheme shows the recently reported papers which applied the coumarin ring system units as a starting material. In 2016, Keshavarzipour et al. described a green approach to coumarin derivatives in the deep eutectic solvent [3]. In addition, owing to the

*Corresponding author:

E-mail address: sajid.m@uokerbala.edu.iq (**S. M. Radhi**); luma.ahmed@uokerbala.edu.iq (**L. M. Ahmed**)

wide application of coumarins, there is considerable interest in the synthesis of coumarins catalyzed by different catalysts [4-13]. Although each of cited methods has its advantages, some of them often suffer from one or more disadvantages such as long reaction times, low yields, hard work-up, and use of hazardous organic solvent.

Due to the importance of the coumarin ring system compounds, in the current study, we hope to describe the one-pot, three component, and green synthesis of 2-(aryl)-3-((2-oxo-2-(2-oxo-2H-chromen-3-yl)ethyl)amino)imidazolidin-4-one derivatives using two different methods including step by step and one-pot methods under microwave irradiation. Over the past decades, some organic reactions were catalyzed by graphene oxide and graphene based catalysts [14-19]. Herein, in the continuation of the nanocatalysts [20-22], we introduce two different methods described for the synthesis of 2-(aryl)-3-((2-oxo-2-(2-oxo-2H-chromen-3-yl)ethyl)amino)imidazolidin-4-one derivatives under microwave irradiation.

2. Experimental

Materials and Apparatus

All chemicals were purchased from Sigma-Aldrich, Fluka, and Merck chemical companies. Microwave reaction has been performed on Shanghai Sineo microwave chemistry technology. Analytical thin layer chromatography (TLC) plate has been done with silica gel 60 F₂₅₄ plates. Melting points have been measured on an Electrothermal Stuart SMP 30 capillary melting point

apparatus and are uncorrected. FT-IR spectra have been recorded using Shimadzu FTIR-8400S Infrared Spectrophotometer as potassium bromide discs. ¹H NMR and ¹³C NMR spectra have been obtained using NMR spectrometer, Bruker, Germany at 500 MHz in DMSO-d₆ as a solvent and TMS as an internal reference at Sharif University of Technology, Tehran, Iran. XRD technique of catalyst was obtained by Philips X'PertPro instrument with 1.54 Å wave lengths of X-ray beam and at a scanning speed of 2° min⁻¹ from 10 to 80 (2θ). The Raman technique was recorded at 532 nm using an Almega Thermo Nicolet Dispersive Raman spectrometer. The SEM images of the catalysts were captured on a Hitachi S4160 instrument. TEM images were captured with a Zeiss-EM10C microscope with an acceleration voltage of 98 kV.

Typically procedure for the synthesis of 3-(2-hydrazinylacetyl)-2H-chromen-2-one (I)

For preparation of 3-(2-hydrazinylacetyl)-2H-chromen-2-one (1), in a 25 mL round bottom flask, a mixture of 3-acetylcoumarin (2.0 mmol, 0.38 g) and 4.0 mL hydrazine in 2.0 mL ethanol as a solvent were heated for 1 h under reflux conditions [31]. The progress of the reaction was checked by TLC. Physical and FT-IR data: yellow solid, with m.p.: 98 °C, yield 90%; FT-IR (cm⁻¹): at 3477.77 and 3412.19 cm⁻¹ (ν sym and asym NH-NH₂ gp), 3084-3057 (ν C-H, benzene), 2928 (ν C-H, aliphatic), 1724.42 (ν C=O, lactone), 1685.84 (ν C=O ketone), 1606.76 (ν C=C, in coumarin).

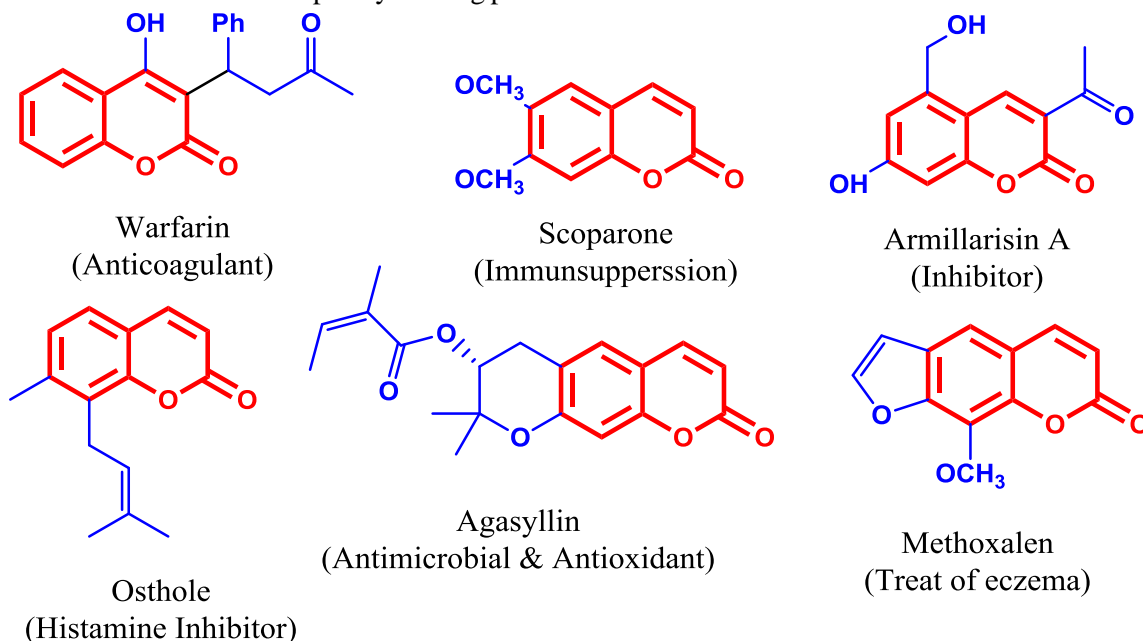
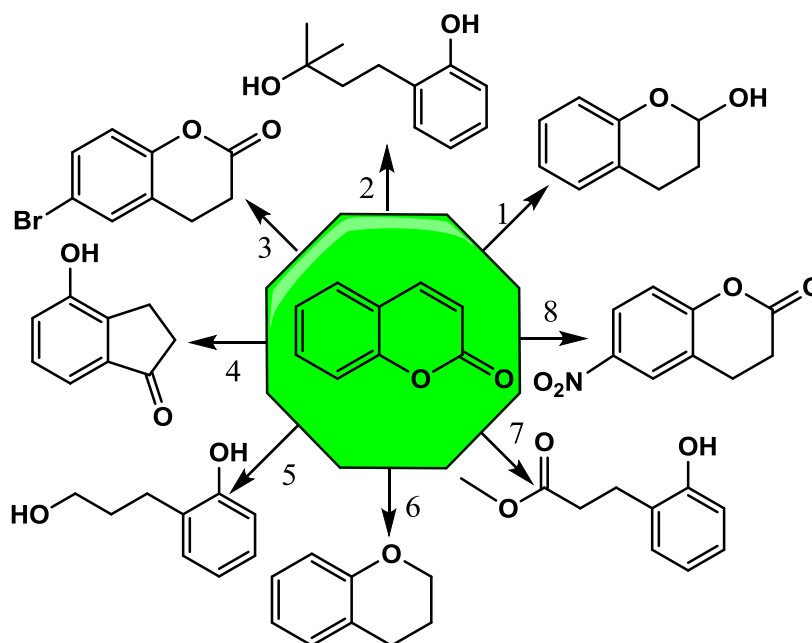


Fig. 1. Some of the important drugs based on coumarin unit



Scheme 1. Different reaction conditions for application of coumarin ring system as starting materials: 1) diisobutylaluminium hydride in hexane, toluene, Time= 1h, T= -78 °C, Yield: 100% [23]. 2) To a solution of dihydrocoumarin (5.0 g, 33.75 mmol) in anhydrous THF (50 mL) at 0 °C, methylmagnesium chloride was added dropwise (101.1 mmol, 33.7 mL, 3.0 M in THF). The reaction mixture was slowly warmed to room temperature and stirred overnight. On completion, the reaction mixture was treated with ice chips containing 25 mL of 1N H₂SO₄. Extraction of the aqueous phase with Et₂O, drying the latter over Na₂SO₄ and concentration under reduced pressure yielded the diol as a white solid (6.07 g, 100%): mp 110-112 °C; TLC R_f 0.37 (EtOAc : Hex, 1:1); ¹H NMR (600 MHz, (CD₃)₂CO) δ 8.22 (broad s, 1H), 7.06-7.07 (m, 1H), 6.97 (m, 1H), 6.77-6.79 (m, 1H), 6.72 (m, 1H), 3.54 (s, 1H), 2.67-2.70 (m, 2H), 1.71-1.73 (m, 2H), 1.22 (s, 6H); ¹³C NMR (400 MHz, (CD₃)₂CO) δ 155.2, 129.9, 129.6, 126.8, 119.6, 115.2, 69.7, 44.1, 29.2, 25.1. Anal. (%) calcd for C₁₁H₁₆O₂ C 73.30, H 8.95; found C 73.28, H 8.97. in tetrahydrofuran, T= 0 - 20 °C, Yield: 100% [24]. 3) aluminum (III) chloride, N-Bromosuccinimide in acetonitrile, Time= 25h, T= 5 - 10 °C, Inert atmosphere, Large scale, Reagent/catalyst, Yield: 91% [25]. 4) aluminum (III) chloride, sodium chloride, T= 200 °C, Inert atmosphere, Yield: 91% [26]. 5) Lithium aluminium tetrahydride in tetrahydrofuran, T= 0 °C, Inert atmosphere, Reflux, Yield: 95% [27]. 6) triethylsilane, indium tribromide in toluene, Yield: 93% [28]. 7) Sulfuric acid, Time= 8h, Heating, Yield: 96% [29]. 8) Nitric acid, acetic anhydride, acetic acid, Time= 1h, T= 20 °C, Yield: 76% [30].

General Procedure for the step by step synthesis of 2-(Aryl)-3-((2-oxo-2-(2-oxo-2H-chromen-3-yl)ethyl)amino)imidazolidin-4-one Derivatives

In a 10 mL round-bottom flask equipped with a condenser in a microwave oven, 1 mmol of 3-(2-hydrazinylacetyl)-2H-chromen-2-one (1), and 1 mmol of aromatic aldehydes in 1 mL of absolute ethanol were irradiated with the power of 325-350 Watt within 3-10 min. The progress of the reaction was monitored using *n*-Hexane: Chloroform: EtOAc (3: 2: 1). After completion of the reactions, the imine products (3a-3h) were obtained and washed with diethyl ether and recrystallized from absolute ethanol. After the successful preparation of imine products (3a-3h), the pointed products were identified by melting point and FT-IR data. Then, 1 mmol of imine products (3a-3h), and 1 mmol of glycine (0.075 g) were irradiated under microwave conditions at 550-600 Watt within 25-30

min. The progress of the reaction was monitored using *n*-Hexane: Chloroform: EtOAc (3: 2: 1). After completion of the reactions, the final products (5a-5h) were obtained and washed with diethyl ether and recrystallized from absolute ethanol.

General Procedure for the synthesis of graphene oxide nanosheets

Graphene oxide nanosheets were prepared by the powder of graphite using a modified Hummer's method [32]. Generally, 10 g of powder of graphite and 5.0 g of NaNO₃ were mixed with 230 mL of H₂SO₄ (98%) in a 5.0 L flask equipped with a condenser in an ice-water (0-3 °C) bath. The materials were mixed using a magnetic stirrer and slowly added 30.0 g of KMnO₄, the mixture was continued for 2.0 h. The materials were moved to a 35 °C water bath and stirred for 0.5 h. Then, about 460 mL of distilled water was slowly added to the flask and the solution temperature increased to 98 °C

and stirred for 0.25 h. Then, 1.4 L of distilled water and 100 mL of hydrogen peroxide (30%) were sequentially added to the material to finish all of the reaction. The dark solution was filtered and washed with 5% HCl solution. The powder of graphite oxide was obtained after drying in a vacuum at 50 °C for 14 h. Then, the graphite oxide was dispersed in water and exfoliated by ultrasound irradiation to generate GO nanosheets, followed by centrifugation to remove unexfoliated graphite oxide.

General Procedure for the one-pot synthesis of 2-(Aryl)-3-((2-oxo-2-(2-oxo-2H-chromen-3-yl)ethyl)amino)imidazolidin-4-one using graphene oxide nanosheets under microwave irradiation

A mixture of 3-(2-hydrazinylacetyl)-2H-chromen-2-one (1) (1 mmol), aromatic aldehyde (2) (2 mmol), and glycine (4) (1.2 mmol) in a tall beaker was irradiated inside a microwave oven in the presence of 15 mg of graphene oxide nanosheets as nanocatalysts. The progress of the reaction was checked by TLC (*n*-hexane: chloroform: ethyl acetate 4: 4: 2). After completion of the reaction, the materials were cooled to room temperature and 30 mL of diethyl ether (6×5 mL) was added. The graphene oxide nanosheets were separated using the vacuum pump. Then, the solution was evaporated by a rotary. After that, the crude products were washed with chloroform (5 mL) and water, to afford the pure products (5a-5h).

General Procedure for the recyclability of graphene oxide nanosheets

At the end of the reaction, the graphene oxide nanosheets were separated and washed thoroughly using water and ethanol. Then, the graphene oxide was dried at 50 °C for 6 h. The reused graphene oxide nanosheets were applied in the one-pot synthesis of 2-(4-chlorophenyl)-5-methyl-3-((2-oxo-2-(2-oxo-2H-chromen-3-yl)ethyl)amino)imidazolidin-4-one (5b) for 7 catalytic cycles.

Selected Spectroscopic and Physical Data

3-(2-(2-(2-hydroxybenzylidene)hydrazinyl)acetyl)-2H-chromen-2-one (3a): Brown Solid, 153 °C, The FT-IR spectrum (cm^{-1}): 3234.73 (ν C- NH gp), 3032.20 (ν C-H, benzene), 2929.97(ν C-H, aliphatic) 1737.92 (ν C=O, lactone), 1680.05(ν C=O ketone), 1610.61 (ν C=N, imine) , 1585.54 (δ C-H, benzene) was done.

3-(2-(2-(4-chlorobenzylidene)hydrazinyl)acetyl)-2H-chromen-2-one (3b): Orange Solid, 142 °C, The FT-IR

spectrum (cm^{-1}): 3340.82 (ν C- NH gp), 3032.20 (ν C-H, benzene), 2839.31(ν C-H, aliphatic), 1739.85 (ν C=O, lactone), 1681.98(ν C=O ketone), 1610.61 (ν C=N, imine) , 1585.54 (δ C-H, benzene) occurred.

3-(2-(2-(4-aminobenzylidene)hydrazinyl)acetyl)-2H-chromen-2-one (3c): Yellow Solid, 162 °C The FT-IR analysis (cm^{-1}): 3304.17 (ν C- NH gp), 3036.06 (ν C-H, benzene), 2931.90(ν C-H, aliphatic), 1728.28 (ν C=O, lactone), 1681.98(ν C=O ketone), 1604.83 (ν C=N, imine) , 1585.54 (δ C-H, benzene) was given.

3-(2-(2-(4-hydroxy-3-methoxybenzylidene)hydrazinyl)acetyl)-2H-chromen-2-one (3d): Yellow Solid, 178 °C, The FT-IR analysis (cm^{-1}): 3437.26 (ν C- OH gp), 3340.82 (ν C- NH gp), 3020.20(ν C-H, benzene), 2929.97 (ν C-H, aliphatic), 1741.97(ν C=O, lactone), 1680.05(ν C=O ketone), 1612.54 (ν C=N, imine), 1585.54 (δ C-H, benzene) was obtained.

2-(2-hydroxyphenyl)-3-((2-oxo-2-(2-oxo-2H-chromen-3-yl)ethyl)amino)imidazolidin-4-one (5a): Yellow Solid, 213 °C The FT-IR analysis (cm^{-1}): 3414.12_{br} (ν O-H and ν N-H, imidazolidine, vib. coupling), 3064.99 (ν C-H, benzene), 1649 (ν C=O and ν N-H, imidazolidine, vib. coupling), 1718.63(ν C=O, lactone), 1608.69(ν C=C, in coumarin); 1H NMR analysis: δ ppm = (3.20, 3.32 Hz, 2H, CH₂ imidazolidine), (4.27 Hz, 1H, CH₂-NH-CH, imidazolidine), (6.27 Hz, 1H, N-CH-N, imidazolidine), 7.15 –7.60 (m, 9H, Ar-H), 8.07 (s, 1H, H-Ar-C=C-), 8.52 (s, 1H, -C=C-H), 7.94 (s, 1H, Ar-O-H) were demonstrated. The signal at 2.82 ppm was assigned to DMSO; ^{13}C NMR analysis: δ ppm = (53.00 Hz, CH₂ imidazolidine), (69.18 Hz, 1H, N-CH-N, imidazolidine), 134.38–117.26(8C-Ar), 147.11(Ar-C=C-) was obtained. The signals at 30.92 ppm were assigned to DMSO.

2-(4-chlorophenyl)-5-methyl-3-((2-oxo-2-(2-oxo-2H-chromen-3-yl)ethyl)amino)imidazolidin-4-one (5b): Black Solid, 203 °C The FT-IR (cm^{-1}): 3348.54 (ν N-H, imidazolidine), 3047.63 (ν C-H, benzene), 1597.11_{br} (ν C=O and ν N-H, imidazolidine, and ν C=C, in coumarin vib. coupling) , 1720.56(ν C=O, lactone) ; 1H NMR analysis: δ ppm = (3.30 , 3.18 Hz, 2H, CH₂ imidazolidine), (3.95 Hz, 1H, CH₂-NH-CH, imidazolidine) , (6.15 Hz, 1H, N-CH-N, imidazolidine), 7.15 –7.60 (m, 8H, Ar-H), 8.07 (s, 1H, H-Ar-C=C-), 8.52 (s, 1H, -C=C-H) were found. The signals at 2.92 ppm were assigned to DMSO; ^{13}C NMR analysis: δ ppm (53.06 Hz, CH₂ imidazolidine), (73.65 Hz, N-CH-N, imidazolidine), 134.38–117.26(8C-Ar) ,

147.13 (Ar-C=C-) were demonstrated. The signals at 30.66 ppm were assigned to DMSO.

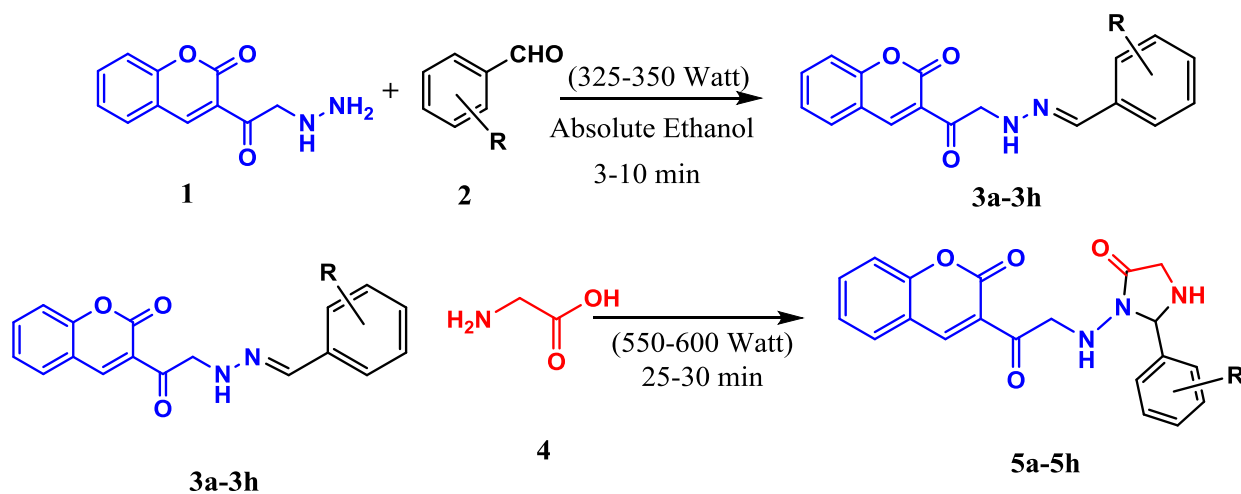
2-(4-aminophenyl)-3-(2-oxo-2-(2-oxo-2H-chromen-3-yl)ethylamino)imidazolidin-4-one (**5c**): Orange Solid, 223 °C The FT-IR spectrum (cm^{-1}): 3350.46 (ν N-H, imidazolidine), 3047.63 (ν C-H, benzene), 1595.18_{br} (ν C=O and ν N-H, imidazolidine, and ν C=C, in coumarin vib. coupling), 1720.56 (ν C=O, lactone); and ¹H NMR analysis: δ ppm = (3.30, 3.18 Hz, 2H, CH₂ imidazolidine), (3.95 Hz, 1H, CH₂-NH-CH, imidazolidine), (6.15 Hz, 1H, N-CH-N, imidazolidine), 7.15–7.60 (m, 8H, Ar-H), 8.07 (s, 1H, H-Ar-C=C-), 8.52 (s, 1H, -C=C-H) were occurred. The signals at 2.79 ppm were assigned to DMSO; ¹³C NMR: δ ppm: (53.03 Hz, CH₂ imidazolidine), (73.42 Hz, N-CH-N, imidazolidine), 134.38–117.26 (8C-Ar), 147.13 (Ar-C=C-). The signals at 30.26 ppm were assigned to DMSO.

2-(3-methoxyphenyl)-3-(2-oxo-2-(2-oxo-2H-chromen-3-yl)ethylamino)imidazolidin-4-one (**5d**): Yellow Solid, 234 °C The FT-IR analysis (cm^{-1}): 3444.98 (ν C-OH gp) 3333.10 (ν N-H, imidazolidine), 3032.20 (ν C-H,

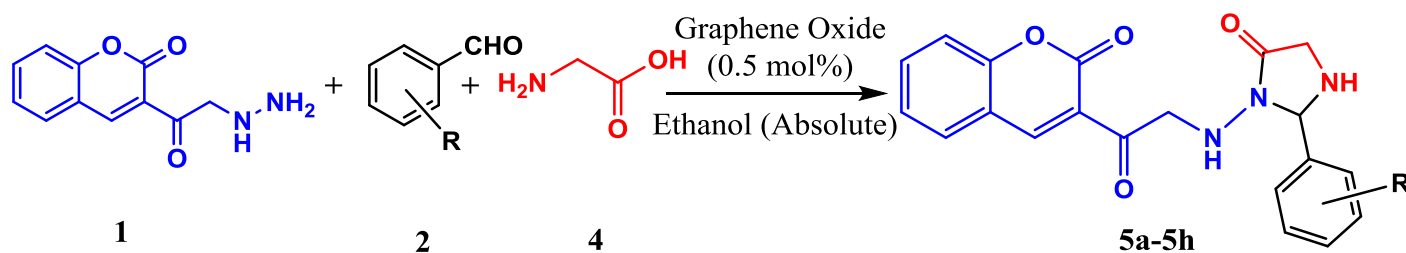
benzene), 1658.84_{br} (ν C=O and ν N-H, imidazolidine vib. coupling), 1724.42 (ν C=O, lactone), 1585.54 (δ C-H, benzene); and ¹H NMR: δ ppm = (3.32, 3.20 Hz, 2H, CH₂ imidazolidine), (3.44 Hz, 1H, CH₂-NH-CH, imidazolidine), (6.58 Hz, 1H, N-CH-N, imidazolidine), 7.15–7.60 (m, 8H, Ar-H), 8.07 (s, 1H, H-Ar-C=C-), 8.52 (s, 1H, -C=C-H) were obtained. The signals at 2.84 ppm were assigned to DMSO; and ¹³C NMR analysis: δ ppm (53.00 Hz, CH₂ imidazolidine), (72.71 Hz, N-CH-N, imidazolidine), 134.38–117.26 (8C-Ar), 147.13 (Ar-C=C-) were produced. The signals at 30.63 ppm were assigned to DMSO.

3. Results and Discussion

The importance of coumarines in pharmaceutical and drug chemistry was previously recognized for several years. Due to the importance of the coumarin based compounds, we want to produce 2-(Aryl)-3-((2-oxo-2-(2-oxo-2H-chromen-3-yl)ethyl)amino)imidazolidin-4-one through the two different approaches including the step by step method under catalyst-free (**Scheme 2**) and one-pot three-component method in the presence of graphene oxide nanosheets (**Scheme 3**).



Scheme 2. Synthesis of 2-(Aryl)-3-((2-oxo-2-(2-oxo-2H-chromen-3-yl)ethyl)amino)imidazolidin-4-one through the step by step approach under catalyst-free conditions.



Scheme 3. One-pot synthesis of 2-(Aryl)-3-((2-oxo-2-(2-oxo-2H-chromen-3-yl)ethyl)amino)imidazolidin-4-one in the presence of graphene oxide nanosheets

Characterization of graphene oxide nanosheets

The graphene oxide nanosheets were prepared for application in the one-pot synthesis of 2-(Aryl)-3-((2-oxo-2-(2-oxo-2H-chromen-3-yl)ethyl)amino)imidazolidin-4-one. The graphene oxide nanosheets were characterized by some techniques including FE-SEM, FT-IR and Raman spectroscopy, XRD spectroscopy, and classical back acid-base titration.

The morphology of graphene oxide nanosheets was shown in **Fig. 2**. The flat and flake-like sheets of nanosheets of graphene oxide were observed in the image of FE-SEM. In addition, in **Fig. 2**, we found that graphene oxide nanosheets consist of aggregated and crumpled thin sheets which are also seen with wrinkles

and folds on the surface of graphene oxide nanosheets. This result indicated that 2D graphene oxide nanosheets may be provided from the exfoliation of graphite oxide powder.

The FT-IR spectrum of graphene oxide nanosheets was shown in **Fig. 3**. Hummer's modification of graphite powder and ultrasound irradiation cuts off the symmetry of graphite powder. The peak at about 1579 cm^{-1} is attributed to carbon-carbon double bonds in the sheets of graphene oxide. Moreover, other peaks at 3362, 2945, 1641, 1174, and 1059 cm^{-1} could be assigned to hydrogen-oxygen, carbon-hydrogen, carbonyl, and carbon-oxygen stretching modes of functional groups such as carboxylic, hydroxyl, and epoxy groups attached to graphene oxide, respectively [33, 34].

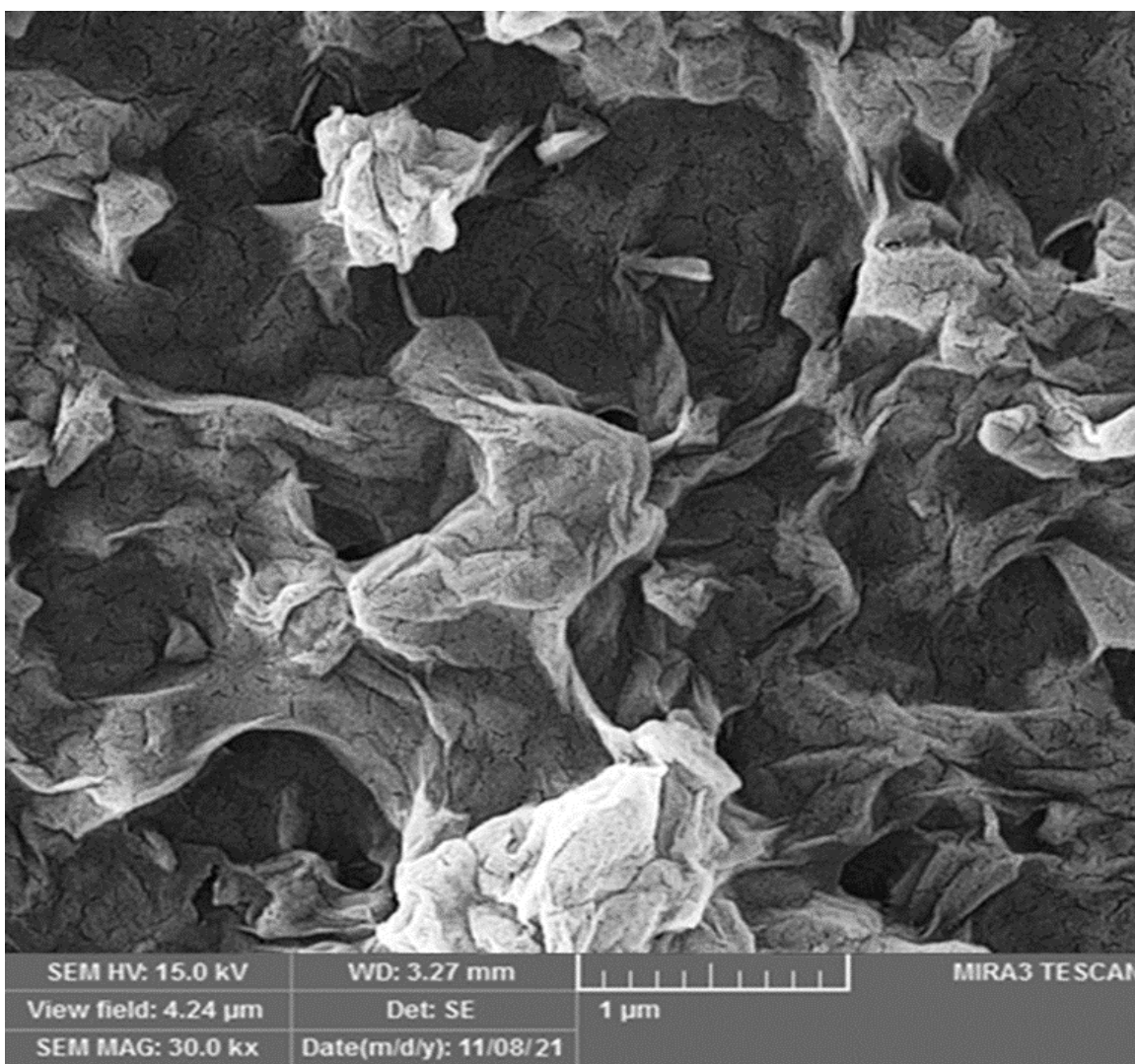


Fig. 2. FE-SEM image of graphene oxide nanosheet

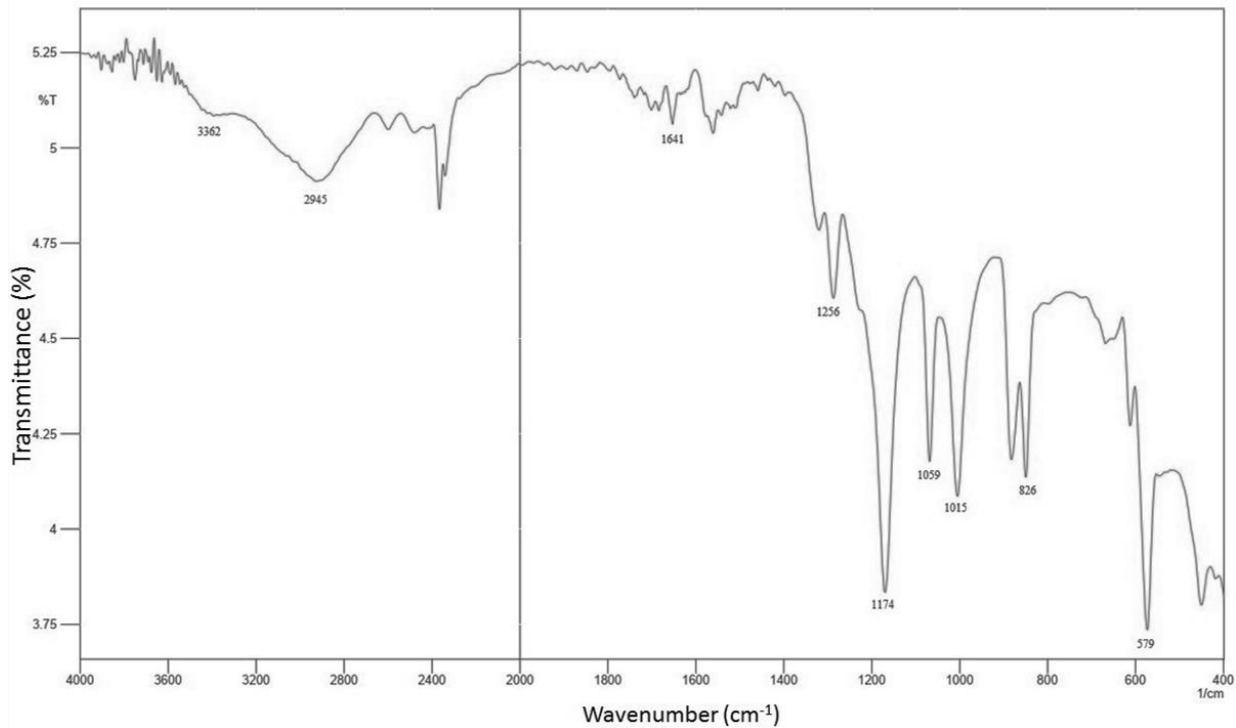


Fig. 3. FT-IR spectrum of graphene oxide nanosheets

Raman spectrum of graphene oxide nanosheet is shown in **Fig. 4**. The peak named D-band is attributed to disorder-induced scattering resulting from the imperfection of disorder graphene sheets. The peak named G-band is related to an E_{2g} mode of graphite and is related to the vibration of sp² hybridized carbon in a 2D nanosheets. The D band is displayed at approximately 1347 cm⁻¹, and the G band appears at

about 1580 cm⁻¹. The G-band increase from the stretching of C-C bond in graphitic powder, and is related to sp² carbon of honey sheets. The D-band is caused by the disordered structure of graphene. The other Raman bands are at 2780 cm⁻¹ (2D band), and 2973 cm⁻¹ (D+G-band) [35].

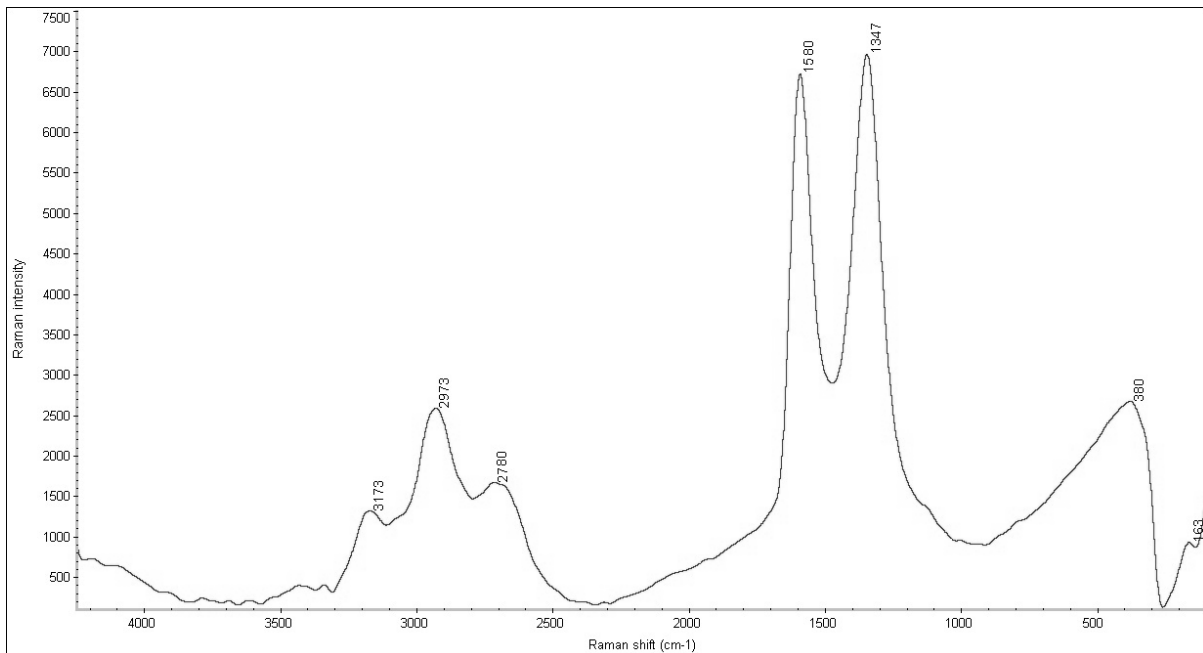


Fig. 4. Raman spectrum of graphene oxide nanosheets

Fig. 5a and **Fig. 5b** show XRD patterns of graphite, and graphene oxide nanosheets. The XRD pattern of graphite (**Fig. 5a**) shows a diffraction peak at about $2\theta=26.3^\circ$ corresponding to the d -spacing of sheets of graphene. After the oxidation process, the peak at about $2\theta=26.3^\circ$ was converted to a broad peak and the peak at $2\theta=12^\circ$ was displayed. The interlayer spacing (d -spacing) of graphene oxide was calculated to be 0.94 nm which revealed the introduction of oxygen functional groups on graphene sheets (**Fig. 5b**) [36].

The density of such as COOH and OH was measured by classical back acid-base titration. The classical back acid-base titration showed that the amount of hydrogen acidic was 5.6 mmol. g^{-1} .

Optimization Synthesis of 2-(Aryl)-3-((2-oxo-2-(2-oxo-2H-chromen-3-yl)ethyl)amino)imidazolidin-4-one Derivatives (step by step method)

To optimize the reaction conditions for the formation of 2-(Aryl)-3-((2-oxo-2-(2-oxo-2H-chromen-3-yl)ethyl)amino)imidazolidin-4-one Derivatives using the step by step method, we applied this optimization using the reaction of 3-(2-hydrazinylacetyl)-2H-chromen-2-one (1) and 4-chlorobenzaldehyde under catalyst-free conditions as a model reaction under microwave irradiation (Step 1) (**Table 1**). In step 2, the glycine was reacted with the final product of step 1 to

obtain the desired product. For finding the appropriate solvent, different solvents including water, methanol, ethanol, and acetonitrile were checked in the model reaction (Table 1, entries 1-4). As shown in this Table, entry 3 gave the best yield for the medium of the model reaction. Therefore, ethanol solvent was selected as a reaction medium. Notably, ethanol is quickly warmed by microwave irradiation [37] For optimization of the power of microwave irradiation, different tests were performed (Table 1, entries 4-6). An increase in power of microwave (325 to 350 Watt) led to the decreased yield of the model reaction and increased time of the desired products. Entry 3 was the best optimum reaction conditions for the synthesis of 2-(Aryl)-3-((2-oxo-2-(2-oxo-2H-chromen-3-yl)ethyl)amino)imidazolidin-4-one Derivatives using step by step method.

Optimization Synthesis of 2-(Aryl)-3-((2-oxo-2-(2-oxo-2H-chromen-3-yl)ethyl)amino)imidazolidin-4-one Derivatives (one-pot method)

To optimize the reaction conditions for the synthesis of 2-(Aryl)-3-((2-oxo-2-(2-oxo-2H-chromen-3-yl)ethyl)amino)imidazolidin-4-one Derivatives using the one-pot method, we applied this optimization using the reaction of 3-(2-hydrazinylacetyl)-2H-chromen-2-one (1), glycine, and 4-chlorobenzaldehyde under microwave conditions in the presence of graphene oxide nanosheets as a model reaction (**Table 2**). Entry 3 was the best condition for the one-pot method.

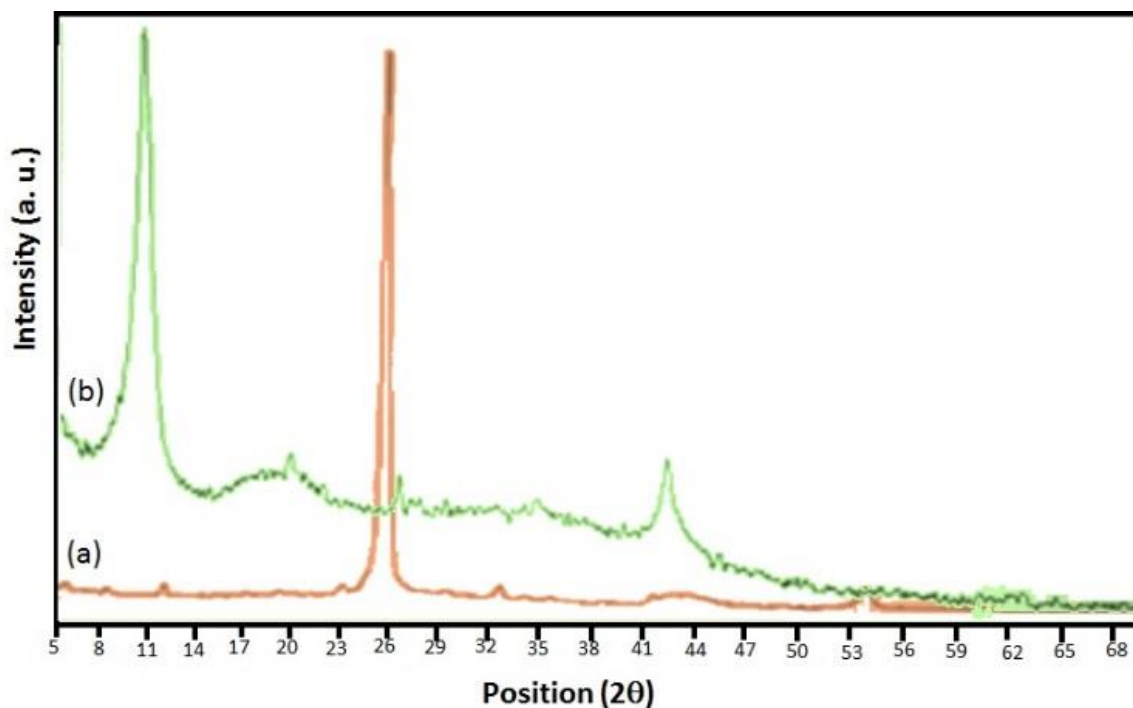
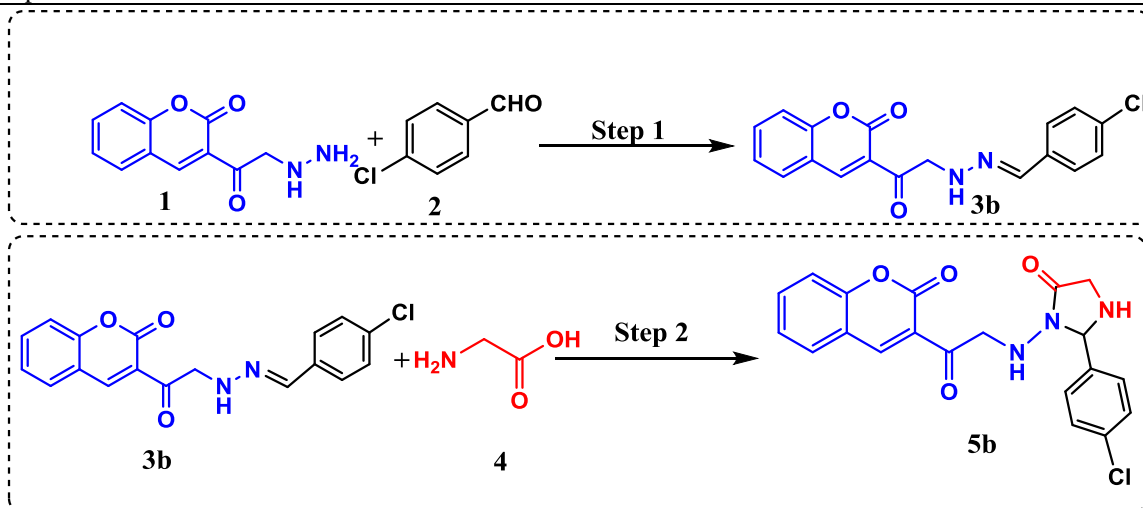
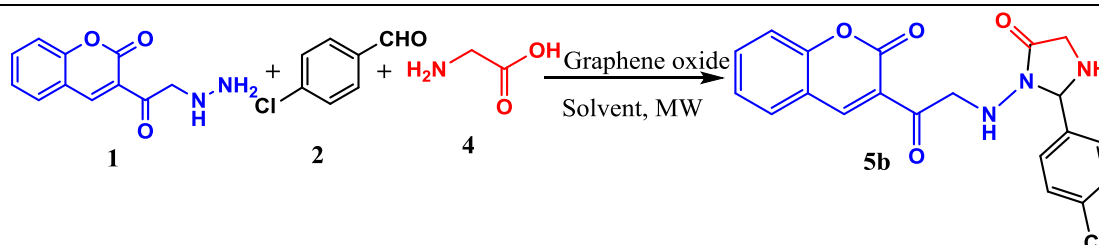


Fig. 5. XRD pattern of a) graphite powder and b) graphene oxide nanosheets

Table 1. Optimization synthesis of 2-(Aryl)-3-((2-oxo-2-(2-oxo-2H-chromen-3-yl)ethyl)amino)imidazolidin-4-one using step by step method^a

Entry	Solvent	Power MW (Watt)	Time (min)	Yield (%) ^b
1	H ₂ O	325	9	69
2	CH ₃ OH	325	12	70
3	C ₂ H ₅ OH	325	5	94
4	CH ₃ CN	325	15	62
5	C ₂ H ₅ OH	300	9	93
6	C ₂ H ₅ OH	350	6	90

a) General reaction conditions: 3-(2-hydrazinylacetyl)-2H-chromen-2-one (1 mmol), 4-chlorobenzaldehyde (1 mmol), glycine (1 mmol), solvent: 1 mL. b) Isolated yield.

Table 2. Optimization synthesis of 2-(Aryl)-3-((2-oxo-2-(2-oxo-2H-chromen-3-yl)ethyl)amino)imidazolidin-4-one using one-pot method^a

Entry	Solvent	Catalyst (mg)	Power MW (Watt)	Glycine (mmol)	Time (min)	Yield (%) ^b
1	H ₂ O	15	300	1.2	13	79
2	CH ₃ OH	15	300	1.2	9	80
3	C ₂ H ₅ OH	15	300	1.2	5	98
4	CH ₃ CN	15	300	1.2	6	82
5	C ₂ H ₅ OH	12	300	1.2	10	85
6	C ₂ H ₅ OH	20	300	1.2	5	95
7	C ₂ H ₅ OH	15	285	1.2	20	68
8	C ₂ H ₅ OH	15	325	1.2	5	91
9	C ₂ H ₅ OH	15	300	1.0	5	86
10	C ₂ H ₅ OH	15	300	1.5	5	97

a) Reaction conditions: 3-(2-hydrazinylacetyl)-2H-chromen-2-one (1 mmol), 4-chlorobenzaldehyde (1 mmol), glycine (x mmol), solvent: 1 mL. b) Isolated yield.

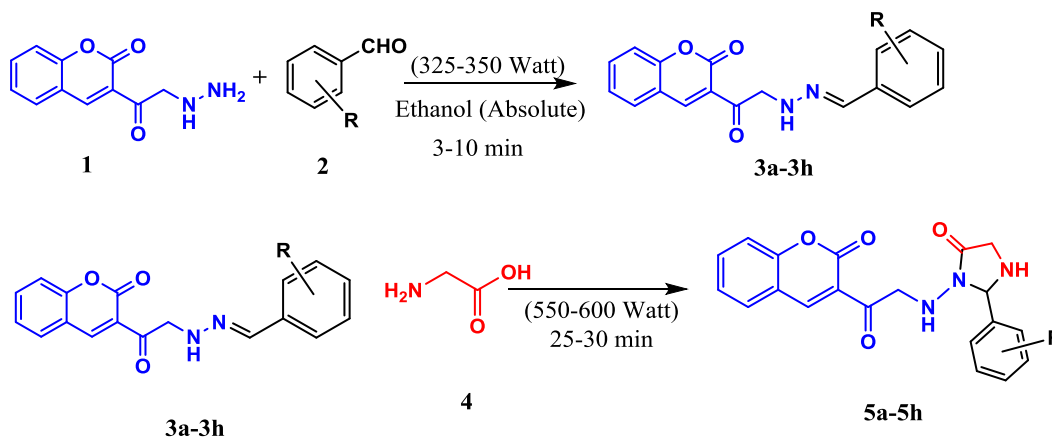
Synthesis of 2-(Aryl)-3-((2-oxo-2-(2-oxo-2H-chromen-3-yl)ethyl)amino)imidazolidin-4-one derivatives

As shown in **Table 3**, a range of aromatic aldehydes was employed to show the applicability and merit of this approach in the synthesis of 2-(Aryl)-3-((2-oxo-2-(2-

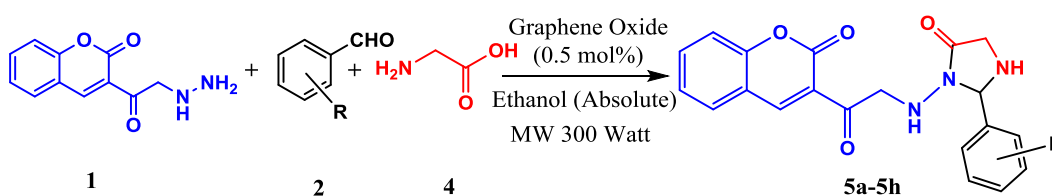
oxo-2H-chromen-3-yl)ethyl)amino)imidazolidin-4-one derivatives using two methods including step by step and one-pot method. To generalize optimum reaction conditions, different derivatives of 2-(Aryl)-3-((2-oxo-2-(2-oxo-2H-chromen-3-yl)ethyl)amino)imidazolidin-4-one were prepared under optimized reaction conditions as discussed above. The reaction via the step-by-step method smoothly proceeded to give the **Table 3**. Synthesis of 2-(Aryl)-3-((2-oxo-2-(2-oxo-2H-chromen-3-yl)ethyl)amino)imidazolidin-4-one derivatives using step by step^a and one-pot^b method

corresponding products in moderate yields and longer reaction times relative to the one-pot method. As can be seen in this Table, the aromatic aldehydes with EW groups on the *ortho*- or *para*- positions accelerated the time of the reaction and improved the yield of desired products compared with ED groups on *ortho*- or *para*-positions of aldehydes.

STEP BY STEP METHOD



ONE-POT METHOD



No	R	Imine Yield (%) ^c (3a-3h)	Product (5a-5h)	Step by Step Method				One-pot Method			
				Time (min)	Yield (%) ^d	TON ^e	TOF (h ⁻¹) ^f	Time (min)	Yield (%) ^d	TON ^e	TOF (h ⁻¹) ^f
1	2-OH	78		26	74	13.2	30.5	6	94	16.8	168.0
2	4-Cl	72		25	65	11.6	27.9	5	98	17.5	218.7
3	4-NH ₂	90		28	83	14.8	31.7	7	89	16.0	133.3

4	3-OCH ₃	69		30	73	13.0	26.0	8	90	16.1	123.8
5	H	85		25	86	15.4	37.0	7	91	16.3	135.8
6	4-Br	81		26	79	14.1	33.9	6	96	16.0	160.0
7	4-NO ₂	68		27	81	14.5	32.2	4	94	16.8	240.0
8	4-F	77		20	89	16.0	48.0	6	95	17.0	170.0

a) General reaction conditions for step by step method: 3-(2-hydrazinylacetyl)-2H-chromen-2-one (1 mmol), aldehyde (1 mmol), glycine (1 mmol), Ethanol: 1 mL. b) General Reaction conditions for one-pot method: 3-(2-hydrazinylacetyl)-2H-chromen-2-one (1 mmol), aldehyde (1 mmol), glycine (1.2 mmol), graphene oxide 15 mg ethanol: 1 mL. c) Isolated yield. d) Isolated yield. e) TON: mmol of the product/mmol of active site of the catalyst. f) TOF: TON/time of the reaction (h).

Fig. 6 displays the reusability of the graphene oxide nanosheets after 7th run. At the end of the reaction, the graphene oxide nanosheets were separated and washed thoroughly using water and ethanol. Then, the graphene oxide was dried at 50 °C for 6 h. The reused graphene oxide nanosheets was applied in the one-pot synthesis of 2-(4-chlorophenyl)-5-methyl-3-((2-oxo-2-(2-oxo-2H-chromen-3-yl)ethyl)amino)imidazolidin-4-one (5b) for 7 catalytic cycles.

In **Scheme 4**, the mechanism of the synthesis of 2-(Aryl)-3-((2-oxo-2-(2-oxo-2H-chromen-3-yl)ethyl)amino)imidazolidin-4-one using step-by-step and one-pot method is presented. Depending on the approach based on step by step or one-pot route, different routes can occur. In step by step route, a condensation reaction between 3-(2-hydrazinylacetyl)-2H-chromen-2-one and aryl aldehyde occurred to produce imine intermediate. Then, 2-aminoacetic acid or glycine attacked to imine intermediate to produce the

final product. In addition, in the one-pot method, two proposed paths could be taken as path A and path B.

4. Conclusions

In conclusion, two different methods were introduced for the synthesis of 2-(aryl)-3-((2-oxo-2-(2-oxo-2H-chromen-3-yl)ethyl)amino)imidazolidin-4-one including the step by step and one-pot methods. Our results showed that the one-pot method was better than step by step method in terms of TON, TOF, time of the reaction, and yield of the reaction. The used catalyst for the one-pot method was graphene oxide nanosheets prepared according to Hummer's method. The graphene oxide nanosheets were characterized by different techniques such as FE-SEM, FT-IR, XRD, and Raman spectroscopy. The graphene oxide nanosheets show the reusability for 7th run without loss of their catalytic activity.

Acknowledgment

The authors are grateful to the University of Kerbala for the financial support of this work.

References

- [1] A.M. Musa, S.J. Cooperwood, F.M.O. Khan, A Review of Coumarin Derivatives in Pharmacotherapy of Breast Cancer, *Curr. Med. Chem.*, 15 (2008) 2664-2679.
- [2] P.A.Z. Hasibuan, U. Harahap, P. Sitorus, D. Satria, The anticancer activities of *Vernonia amygdalina* Delile. Leaves on 4T1 breast cancer cells through phosphoinositide 3-kinase (PI3K) pathway, *Heliyon*, 6 (2020) e04449.
- [3] F. Keshavarzipour, H. Tavakol, The synthesis of coumarin derivatives using choline chloride/zinc chloride as a deep eutectic solvent, *J. Iran. Chem. Soc.*, 13 (2016) 149-153.
- [4] M. Hosseini-Sarvari, S. Najafvand-Derikvandi, Synthesis of 4-(trifluoromethyl) coumarins using nano sulfated-titania as solid acid catalyst under solvent-free conditions, *Iran. J. Catal.*, 6 (2016) 423-430.
- [5] A.R. Hajipour, N. Sheikhan, M.A. Alaei, A. Zarei, Brønsted acidic ionic liquid as the efficient and reusable catalyst for synthesis of coumarins via Pechmann condensation under solvent-free conditions, *Iran. J. Catal.*, 5 (2015) 231-236.
- [6] K. Niknam, S.A. Sajadi, R. Hosseini, M. Baghernejad, Silica-bonded *n*-propyldiethylenetriamine sulfamic acid as a recyclable solid acid catalyst for the synthesis of coumarin and biscoumarin derivatives, *Iran. J. Catal.*, 4 (2014) 163-173.
- [7] S.S. Gholap, U.P. Deshmukh, M.S. Tambe, Synthesis and in-vitro antimicrobial screening of 3-cinnamoyl coumarin and 3-[3-(1H-indol-2-yl)-3-aryl-propanoyl]-2H-chromen-2-ones, *Iran. J. Catal.*, 3 (2013) 171-176.
- [8] J. Banothu, R. Bavantula, P.A. Crooks, Facile one-pot multicomponent synthesis of 2-amino-6-(2-oxo-2H-chromen-3-yl)-4-arylpyridine-3-carbonitriles using Brønsted acidic ionic liquid as catalyst under solvent-free conditions, *Iran. J. Catal.*, 3 (2013) 41-47.
- [9] M.R. Antonijević, D.M. Simijonović, E.H. Avdović, A. Ćirić, Z.D. Petrović, J.D. Marković, V. Stepanić, Z.S. Marković, Green One-Pot Synthesis of Coumarin-Hydroxybenzohydrazide Hybrids and Their Antioxidant Potency, *Antioxidants*, 10 (2021) 1106.
- [10] B. Borah, K.D. Dwivedi, B. Kumar, L.R. Chowhan, Recent advances in the microwave- and ultrasound-assisted green synthesis of coumarin-heterocycles, *Arabian Journal of Chemistry*, 15 (2022) 103654.
- [11] G. Yang, L. Shi, Z. Pan, L. Wu, L. Fan, C. Wang, C. Xu, J. Liang, The synthesis of coumarin thiazoles containing a trifluoromethyl group and their antifungal activities, *Arabian Journal of Chemistry*, 14 (2021) 102880.
- [12] P. Gong, Y. Ma, X. Wang, L. Yu, S. Zhu, A facile and diverse synthesis of coumarin substituted spirooxindole and dispiro oxindole-pyrrolizidine/pyrrolothiazole/pyrrolidine derivatives via 1, 3-dipolar cycloaddition, *Tetrahedron*, 91 (2021) 132221.

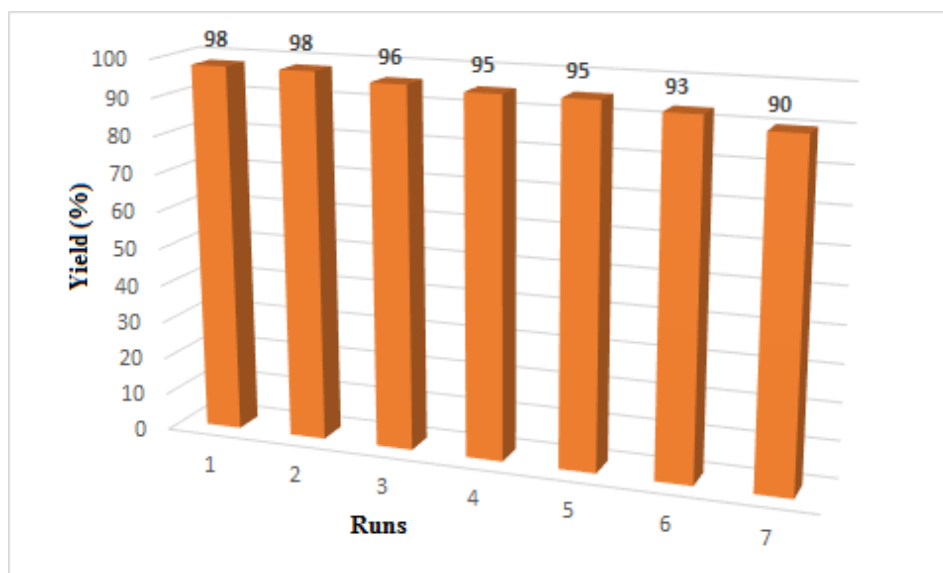
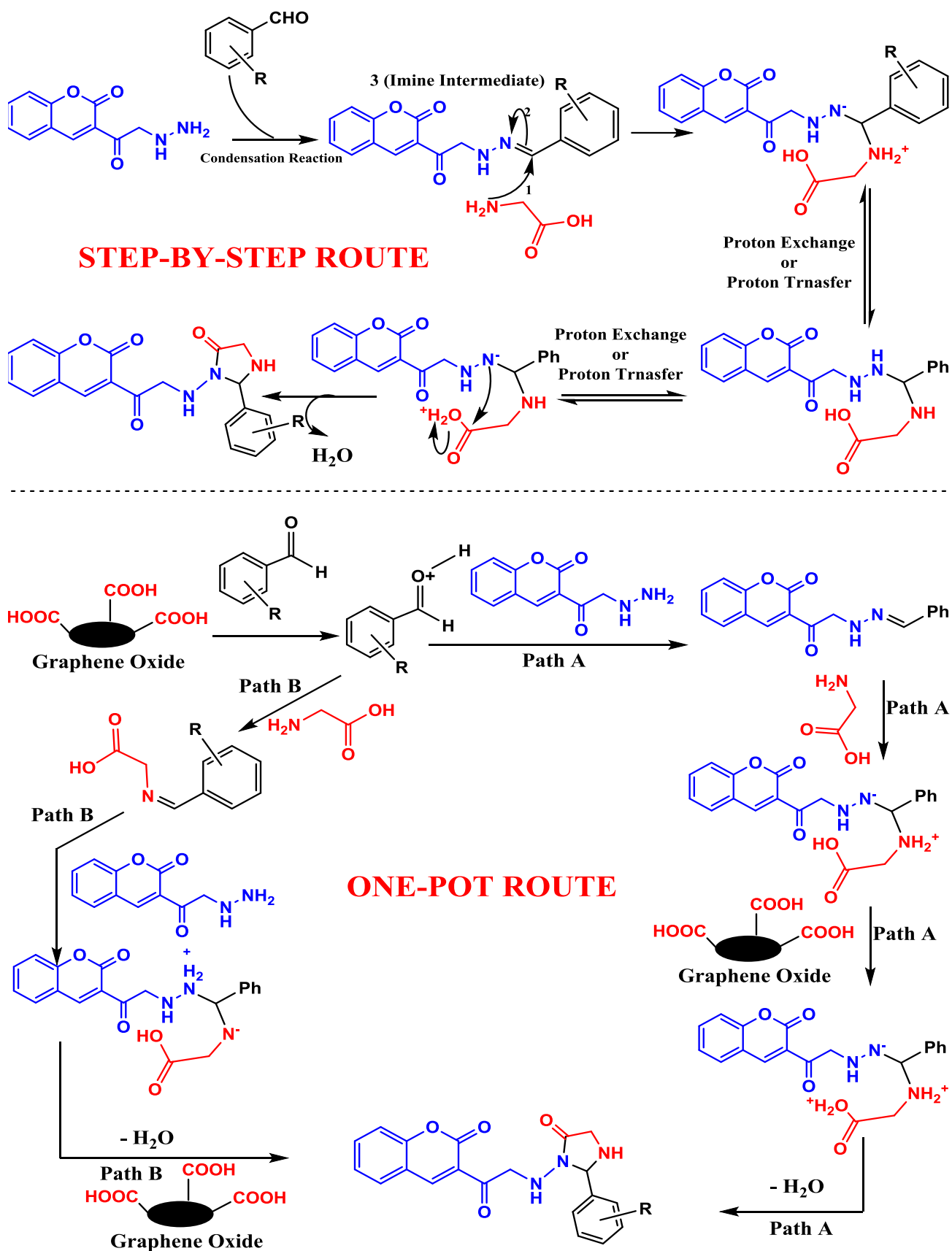


Fig. 6. Reusability of graphene oxide nanosheets in the synthesis of 2-(4-chlorophenyl)-5-methyl-3-((2-oxo-2-(2-oxo-2H-chromen-3-yl)ethyl)amino)imidazolidin-4-one under microwave irradiation.



Scheme 4. A reasonable mechanism route for the two routes including step-by-step and one-pot methods

- [13] P. Bhaumick, L.H. Choudhury, Multicomponent click polymerization for the synthesis of coumarin containing 1,4-polytriazoles and their application as dye adsorbent, *Polymer*, 243 (2022) 124580.
- [14] A. Jiříčková, O. Jankovský, Z. Sofer, D. Sedmidubský, Synthesis and Applications of Graphene Oxide, *Materials*, 15 (2022) 920.
- [15] M. Verma, I. Lee, J. Oh, V. Kumar, H. Kim, Synthesis of EDTA-functionalized graphene oxide-chitosan nanocomposite for simultaneous removal of inorganic and organic pollutants from complex wastewater, *Chemosphere*, 287 (2022) 132385.
- [16] M. Mirza-Aghayan, M. Mohammadi, R. Boukherroub, Synthesis and characterization of palladium nanoparticles immobilized on graphene oxide functionalized with triethylenetetramine or 2,6-diaminopyridine and application for the Suzuki cross-coupling reaction, *J. Organomet. Chem.*, 957 (2022) 122160.
- [17] G. Venkatesh, R. Suganesh, J. Jayaprakash, M. Srinivasan, K.M. Prabu, Perovskite type BaSnO₃-reduced graphene oxide nanocomposite for photocatalytic decolorization of organic dye pollutant, *Chem. Phys. Lett.*, 787 (2022) 139237.
- [18] Q. Ma, J. Ming, X. Sun, N. Liu, G. Chen, Y. Yang, Visible light active graphene oxide modified Ag/Ag₂O/BiPO₄/Bi₂WO₆ for photocatalytic removal of organic pollutants and bacteria in wastewater, *Chemosphere*, 306 (2022) 135512.
- [19] S. Peng, Y. Huang, S. Ouyang, J. Huang, Y. Shi, Y.-J. Tong, X. Zhao, N. Li, J. Zheng, J. Zheng, X. Gong, J. Xu, F. Zhu, G. Ouyang, Efficient solid phase microextraction of organic pollutants based on graphene oxide/chitosan aerogel, *Anal. Chim. Acta*, 1195 (2022) 339462.
- [20] E.N. Alkhafaji, N.A. Oda, L.M. Ahmed, Characterization of silver nanohybrid with layers double hydroxide and demonstration inhibition of antibiotic-resistance *Staphylococcus aureus*, *Egyptian Journal of Chemistry*, 65 (2022) 1-2.
- [21] H. Kadhim, L. Ahmed, M. AL-Hachamii, Facile Synthesis of Spinel CoCr₂O₄ and Its Nanocomposite with ZrO₂: Employing in Photo-catalytic Decolorization of Fe (II)-(luminol-Tyrosine) Complex, *Egyptian Journal of Chemistry*, 65 (2022) 481-488.
- [22] B. Hasan Taresh, F. Hadi Fakhri, L. M. Ahmed, Synthesis and Characterization of CuO/CeO₂ Nanocomposites and Investigation Their Photocatalytic Activity, *Journal of Nanostructures*, 12 (2022) 563-570.
- [23] J.M. Casas-Solvas, J.D. Howgego, A.P. Davis, Synthesis of substituted pyrenes by indirect methods, *Org. Biomol. Chem.*, 12 (2014) 212-232.
- [24] R. Jetson, N. Malik, A. Luniwal, V. Chari, M. Ratnam, P. Erhardt, Practical synthesis of a chromene analog for use as a retinoic acid receptor alpha antagonist lead compound, *Eur. J. Med. Chem.*, 63 (2013) 104-108.
- [25] F. Peng, L. Tan, L. Chen, S.M. Dalby, D.A. DiRocco, J. Duan, M. Feng, G. Gong, H. Guo, J.C. Hethcox, L. Jin, H.C. Johnson, J. Kim, D. Le, Y. Lin, W. Liu, J. Shen, Y. Wan, C. Xiao, B. Xiang, Q. Xiang, J. Xu, L. Yan, W. Yang, H. Ye, Y. Yu, J. Zhang, Manufacturing Process Development for Belzutifan, Part 1: A Concise Synthesis of the Indanone Starting Material, *Org. Process Res. Dev.*, 26 (2022) 508-515.
- [26] P. Leowanawat, N. Zhang, V. Percec, Nickel Catalyzed Cross-Coupling of Aryl C–O Based Electrophiles with Aryl Neopentylglycolboronates, *J. Org. Chem.*, 77 (2012) 1018-1025.
- [27] B.I. Gaiser, M. Danielsen, E. Marcher-Rørsted, K. Røpke Jørgensen, T.M. Wróbel, M. Frykman, H. Johansson, H. Bräuner-Osborne, D.E. Gloriam, J.M. Mathiesen, D. Sejer Pedersen, Probing the Existence of a Metastable Binding Site at the β 2-Adrenergic Receptor with Homobivalent Bitopic Ligands, *J. Med. Chem.*, 62 (2019) 7806-7839.
- [28] R. Lagoutte, J.A. Wilkinson, A novel one-step method for the reductive allylation of esters and the first total synthesis of (\pm)-erythroccamide B, *Tetrahedron Lett.*, 51 (2010) 6942-6944.
- [29] A. Kleineweischede, J. Mattay, Synthesis of Amino- and Bis(bromomethyl)-Substituted Bi- and Tetradentate N-Heteroaromatic Ligands: Building Blocks for Pyrazino-Functionalized Fullerene Dyads, *Eur. J. Org. Chem.*, 2006 (2006) 947-957.
- [30] A.R. Katritzky, F.-B. Ji, W.-Q. Fan, P. Beretta, M. Bertoldi, Syntheses of triazolo[6,7-d]phthalide and triazolo[6,7-d]dihydrocoumarin, *J. Heterocycl. Chem.*, 29 (1992) 1519-1523.
- [31] K. Jakhar, J. Makrandi, A green synthesis and antibacterial activity of 2-aryl-5-(coumarin-3-yl)-thiazolo [3, 2-b][1, 2, 4] triazoles, *Indian J. Chem.*, 15B (2012) 1511-1516.
- [32] W.S. Hummers, R.E. Offeman, Preparation of Graphitic Oxide, *J. Am. Chem. Soc.*, 80 (1958) 1339-1339.
- [33] A. Razaq, F. Bibi, X. Zheng, R. Papadakis, S.H.M. Jafri, H. Li, Review on Graphene-, Graphene Oxide-, Reduced Graphene Oxide-Based Flexible Composites: From Fabrication to Applications, *Materials*, 15 (2022) 1012.

- [34] Y. Zhu, S. Murali, W. Cai, X. Li, J.W. Suk, J.R. Potts, R.S. Ruoff, Graphene and Graphene Oxide: Synthesis, Properties, and Applications, *Adv. Mater.*, 22 (2010) 3906-3924.
- [35] K.N. Kudin, B. Ozbas, H.C. Schniepp, R.K. Prud'homme, I.A. Aksay, R. Car, Raman Spectra of Graphite Oxide and Functionalized Graphene Sheets, *Nano Lett.*, 8 (2007) 36-41.
- [36] D. Long, W. Li, L. Ling, J. Miyawaki, I. Mochida, S.-H. Yoon, Preparation of nitrogen-doped graphene sheets by a combined chemical and hydrothermal reduction of graphene oxide, *Langmuir*, 26 (2010) 16096-16102.
- [37] X. Wu, M. Larhed, Microwave-Enhanced Aminocarbonylations in Water, *Org. Lett.*, 7 (2005) 3327-3329.